

Nucleon to $\Delta(1232)$ Resonance Transition Form Factors from Lattice QCD

Srijit Paul,^{a,*} Luka Leskovec,^b Stefan Meinel,^c John W. Negele,^d Ferenc Pittler^e
and Andrew V. Pochinsky^d

^aMaryland Center for Theoretical Physics, University of Maryland, College Park, USA

^bJöze Stefan Institute, Jamova 39, 1000 Ljubljana, Slovenia

^cDepartment of Physics, University of Arizona, Tucson, AZ 85721, USA

^dCenter for Theoretical Physics, Massachusetts Institute of Technology, Cambridge, MA 02139, USA

^eComputation-based Science and Technology Research Center, The Cyprus Institute, 20 Kavafi Str., Nicosia 2121, Cyprus

E-mail: spaul137@umd.edu

We present progress in a lattice QCD study of the electromagnetic and axial $N \rightarrow \Delta(1232)$ resonance transition form factors. Our long-term aim is to apply the Lellouch-Lüscher formalism to extract infinite-volume $N \rightarrow N\pi$ form factors from finite-volume matrix elements. We previously computed the required $N\pi$ scattering amplitudes on an ensemble with $N_f = 2 + 1$ clover fermions at $m_\pi \approx 255$ MeV and $L \approx 2.8$ fm, and obtained the Δ resonance parameters $m_\Delta = 1378(11)$ MeV and $g_{\Delta-N\pi} = 23.8(2.8)$. We have now additionally computed the three-point functions for six source-sink separations ranging from $t_{\text{sep}} = 0.7 - 1.2$ fm. Here, we present a first look at the three-point functions data by extracting the $N \rightarrow \Delta$ transition form factors using the single-hadron approach.

*The 42nd International Symposium on Lattice Field Theory, LATTICE 2025
2nd-8th November, 2025 Mumbai,
India*

*Speaker

1. Introduction

Nucleon resonances play a pivotal role in our understanding of the strong interactions. The lowest-lying baryon resonance, the $\Delta(1232)$, dominates pion production in the few-hundred-MeV energy range and provides a clean window into deformation effects and testing the non-perturbative nature of the pion-cloud contributions [1, 2]. The axial $N \rightarrow \Delta$ transition plays an equally important role in neutrino-induced pion production and therefore in the modeling of systematic uncertainties for neutrino-nucleus cross-sections at DUNE [3]. Experiments such as CLAS at Jefferson Lab [4], A1 and A2 Collaborations at MAMI Mainz [5] have studied the $N \rightarrow \Delta$ transition for decades. However, the interpretation of these experiments is complicated by the fact that the $\Delta(1232)$ is a resonance in the $N\pi$ channel, and thus the transition form factors are not directly related to single-hadron matrix elements. From theoretical point of view, there have been first principles approaches with a caveat that $\Delta(1232)$ is treated as a stable hadron [6–10]. Recently, in the axial sector, there has been a marked disagreement in the prediction of C_3^A between continuum quark–diquark Faddeev approach and phenomenological model predictions [11]. This demands a first-principles determination of the $N \rightarrow \Delta$ transition form factors from lattice QCD where the Δ is treated as a resonance, in order to resolve this tension and to provide a benchmark for the phenomenological models and experiments.

Our long-term program is to compute the infinite-volume $N \rightarrow N\pi$ matrix elements for both vector and axial currents in the $I = 3/2$, p -wave channel, and to extract the corresponding $N \rightarrow \Delta$ resonance transition form factors from these amplitudes. As a prerequisite, we previously determined the required $N\pi$ scattering amplitudes on an $N_f = 2 + 1$ clover ensemble with $m_\pi \approx 255$ MeV and $L \approx 2.8$ fm, obtaining the Δ resonance parameters [12].

In these proceedings we report our current progress on the three-point functions needed for the transition form factors. We have computed the relevant correlation functions for six source–sink separations in the range $t_{\text{sep}} = 0.7\text{--}1.2$ fm. As a first look at the data, we extract the $N \rightarrow \Delta$ transition form factors using the conventional single-hadron approach (treating the Δ as an isolated state) to test the statistical quality of the data for applying the analysis pipeline. These results are an intermediate step toward the full finite-volume formalism for $N \rightarrow N\pi$ matrix elements.

2. Methodology

Lattice Setup: We perform our calculations on a $N_f = 2 + 1$ ensemble generated by the Budapest-Marseille-Wuppertal collaboration where the gluon action is the tree-level Symanzik improved gauge action and the fermion action is a clover-improved Wilson action with the gauge links in it smeared using two levels of HEX smearing [13]. In our previous work [12], we determined the Δ resonance parameters on this ensemble, which are required for the analysis of the transition form factors. The parameters of the ensemble are summarized in Table 1. The scale setting had been performed using the Ω baryon mass.

Smearing and Interpolating Operators: We perform the calculation with a randomly chosen Wuppertal-smeared source position on each time slice of the lattice. The smearing parameters are $\alpha = 3.0$ and $N_{\text{Wup}} = 45$. We use the standard single hadron interpolating operator for the pion and the delta, and for the nucleon we use both the standard $C\gamma_5$ and $C\gamma_0\gamma_5$ for the diquark component

Label	$N_s^3 \times N_t$	β	am_l	a (fm)	m_π (MeV)	$m_\pi L$
A7	$24^3 \times 48$	3.31	-0.09530	0.116	258.3(1.1)	3.6

Table 1: Parameters of the lattice gauge-field ensembles A7.

as shown in the following equations:

$$\pi(\vec{p}) = \sum_{\vec{x}} \bar{d}(\vec{x}) \gamma_5 u(\vec{x}) e^{i\vec{p}\cdot\vec{x}}, \quad (1)$$

$$N_\alpha^{(1)}(\vec{p}) = \sum_{\vec{x}} \epsilon_{abc} u_a(\vec{x})_\alpha \left(u_b^T(\vec{x}) C \gamma_5 d_c(\vec{x}) \right) e^{i\vec{p}\cdot\vec{x}}, \quad (2)$$

$$N_\alpha^{(2)}(\vec{p}) = \sum_{\vec{x}} \epsilon_{abc} u_a(\vec{x})_\alpha \left(u_b^T(\vec{x}) C \gamma_0 \gamma_5 d_c(\vec{x}) \right) e^{i\vec{p}\cdot\vec{x}}, \quad (3)$$

$$\Delta_{\alpha i}^+(\vec{p}) = \sum_{\vec{x}} \frac{1}{\sqrt{3}} \epsilon_{abc} \left\{ 2 \left[u_a^T C \gamma_i d_b \right] u_{c,\alpha} + \left[u_a^T C \gamma_i u_b(\vec{x}) \right] d_{c,\alpha} \right\} e^{i\vec{p}\cdot\vec{x}}. \quad (4)$$

The bilocal $N\pi$ interpolating operators are constructed as products of the single-hadron operators with the appropriate Clebsch-Gordan coefficients to project onto the $I = 3/2$, P -wave channel.

Infinite-Volume Matrix Elements: The $N \rightarrow \Delta$ transition form factors are defined through the matrix elements of the current between the nucleon and the $N\pi$ states projected onto the P -wave channel with $I = \frac{3}{2}$ and the total $J = \frac{3}{2}^+$. In the single-hadron approach, these are extracted from three-point functions with a Δ interpolating operator at the source, a nucleon interpolating operator at the sink, and an insertion of either the vector or axial current at an intermediate time slice. This can be represented for the vector current as,

$$\langle \Delta(\mathbf{p}', s') | j_\mu^{\text{em}} | N(\mathbf{p}, s) \rangle = N \bar{u}_\sigma(\mathbf{p}', s') \Gamma_{\sigma\mu} u(\mathbf{p}, s) \quad (5)$$

with $j_\mu^{\text{em}} = \left[\frac{2}{3} \bar{u} \gamma_\mu u - \frac{1}{3} \bar{d} \gamma_\mu d \right]$ representing the vector current, and $N \equiv N(m_\Delta, m_N, E_\Delta(\mathbf{p}'), E_N(\mathbf{p}))$ is a kinematic factor. This is the point where one can distinguish the single-hadron approach where the Δ is treated as a stable ground state and the multi-hadron finite volume Lellouch-Lüscher approach where the Δ is treated as a resonance in the $N\pi$ channel.

Δ as stable($1 \rightarrow 1$): Using the Jones and Scadron decomposition, employing Rarita-Schwinger on mass shell constraints for the Δ , Lorentz covariance and current conservation, the Lorentz-covariant vertex (tensor) $\Gamma_{\sigma\mu}$ can be expressed in terms of three vector form factors G_M^* , G_E^* and G_C^* as follows:

$$\mathcal{O}_{\sigma\mu} = G_M^*(q^2) K_{\sigma\mu}^M + G_E^*(q^2) K_{\sigma\mu}^E + G_C^*(q^2) K_{\sigma\mu}^C \quad (6)$$

where $K_{\sigma\mu}^M$, $K_{\sigma\mu}^E$ and $K_{\sigma\mu}^C$ are the magnetic dipole, electric quadrupole and Coulomb quadrupole kinematic factors respectively.

Δ as resonance($1 \rightarrow 2$): In the multi-hadron approach, the Δ is treated as a resonance in the $N\pi$ channel, therefore we can't use the Rarita-Schwinger on mass shell constraints for the Δ . In the multi-hadron approach, the $N \rightarrow \Delta$ transition after partial wave projection to the $\ell = 1$ channel can be expressed as 3 independent form factors close to the resonance pole [14].

The distinction between the single-hadron and multi-hadron approaches is the extracted form factors are a function of q^2 in the single-hadron approach, while they are a function of both q^2 and the $N\pi$ invariant mass $\sqrt{s_{N\pi}}$ in the multi-hadron approach. In our approach to extract the $N \rightarrow \Delta$ transition form factors, we will first extract the Jones-Scadron form factors using the single-hadron approach to test the signal quality and to validate the analysis pipeline. We will then extract the helicity form factors using the multi-hadron approach and apply the Lellouch-Lüscher formalism to relate these to infinite-volume $N \rightarrow N\pi$ transition amplitudes.

Correlation Functions and Analysis: We compute the three-point functions for six source-sink separations in the range $t_{\text{sep}} = 0.7\text{--}1.2$ fm, given by the following expression for the vector current,

$$G_i^{\Delta j^{\mu N}}(t_2, t_1; \vec{p}', \vec{p}; \Gamma) = \sum_{\vec{x}_2, \vec{x}_1} e^{-i\vec{x}_2 \cdot \vec{p}} \langle 0 | \Gamma^{\beta\alpha} \Delta_{\alpha,i}(\vec{0}, 0) j_{\mu}(\vec{x}_1, t_1) \bar{N}_{\beta}(\vec{x}_2, t_2) | 0 \rangle e^{-i\vec{x}_1 \cdot (\vec{p}' - \vec{p})}, \quad (7)$$

where Γ is a projection matrix in Dirac space. There is just one topology for the three-point function in the single-hadron approach as shown in Fig. 1. This is computed using combination of point-to-all and sequential propagators. Once we have the three-point functions, we construct

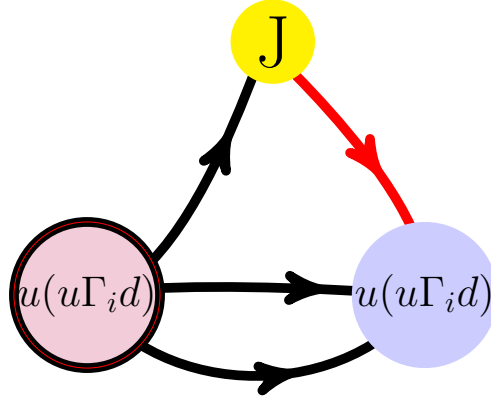


Figure 1: The three-point function topology for the single-hadron approach. The point source is represented by the red bounded circle and the point-to-all propagator is represented by the blackline. The sequential source is the current insertion represented by the yellow circle and the sequential propagator is represented by the red line. The nucleon sink is represented by the blue circle.

the following symmetric ratios to cancel out the unknown overlap factors and the exponential time dependence,

$$R_{\sigma}^{\text{sym}}(t_2, t_1; \mathbf{p}', \mathbf{p}; \Gamma; \mu) = \left[\frac{\langle G_{\sigma}^{\Delta j^{\mu N}}(t_2, t_1; \mathbf{p}', \mathbf{p}; \Gamma) \rangle \langle G_{\sigma}^{N j^{\mu \Delta}}(t_2, t_1; -\mathbf{p}, -\mathbf{p}'; \Gamma^{\dagger}) \rangle}{\langle \delta_{ij} G_{ij}^{\Delta \Delta}(t_2, \mathbf{p}'; \Gamma_4) \rangle \langle G^{NN}(t_2, -\mathbf{p}; \Gamma_4) \rangle} \right]^{1/2}, \quad (8)$$

$$\xrightarrow[t_2-t_1 \gg \text{large}, t_1 \gg \text{large}]{} |\Pi_{\sigma}(\mathbf{p}', \mathbf{p}; \Gamma; \mu)| \quad (9)$$

where $G_{ij}^{\Delta\Delta}$ and G^{NN} are the two-point functions for the Δ and the nucleon respectively. The ratio is constructed such that it approaches a constant $\Pi_\sigma(\mathbf{p}', \mathbf{p}; \Gamma; \mu)$ in the limit of large time separations, which can be related to the transition form factors through the matrix element definition in Eq. 5. One caveat of the symmetric definition of the ratio is that it loses information about the sign of the 3-point function. In order to retain the sign information, we define the following asymmetric ratio,

$$R_\sigma^{sign}(t_2, t_1; \mathbf{p}', \mathbf{p}; \Gamma; \mu) \quad (10)$$

$$= \frac{\langle G_\sigma^{\Delta J \mu N}(t_2, t_1; \mathbf{p}', \mathbf{p}; \Gamma) \rangle}{\langle G_{ii}^{\Delta\Delta}(t_2, \mathbf{p}'; \Gamma_4) \rangle} \left[\frac{\langle G_{ii}^{\Delta\Delta}(t_2, \mathbf{p}'; \Gamma_4) \rangle \langle G^{NN}(t_2 - t_1, \mathbf{p}; \Gamma_4) \rangle \langle G_{ii}^{\Delta\Delta}(t_1, \mathbf{p}'; \Gamma_4) \rangle}{\langle G^{NN}(t_2, \mathbf{p}; \Gamma_4) \rangle \langle G_{ii}^{\Delta\Delta}(t_2 - t_1, \mathbf{p}'; \Gamma_4) \rangle \langle G^{NN}(t_1, \mathbf{p}; \Gamma_4) \rangle} \right]^{1/2} \quad (11)$$

and compute the sign of the symmetric ratio to construct the signed ratio,

$$R_\sigma(t_2, t_1; \mathbf{p}', \mathbf{p}; \Gamma; \mu) = R_\sigma^{sym}(t_2, t_1; \mathbf{p}', \mathbf{p}; \Gamma; \mu) \times \text{sign} \left(R_\sigma^{sign}(t_2, t_1; \mathbf{p}', \mathbf{p}; \Gamma; \mu) \right) \quad (12)$$

$$\stackrel{t_2 - t_1 \gg 1, t_1 \gg 1}{\Rightarrow} \Pi_\sigma(\mathbf{p}', \mathbf{p}; \Gamma; \mu) \quad (13)$$

For the preliminary analysis, we perform a plateau fit to the central 3 time slices for the 3 highest source-sink separations of this ratio $R_\sigma(t_2, t_1; \mathbf{p}', \mathbf{p}; \Gamma; \mu)$ to extract the transition form factors. Now we use the matrix element definition in Eq.(5) to relate the extracted $\Pi_\sigma(\mathbf{p}', \mathbf{p}; \Gamma; \mu)$ to the transition form factors. In the single-hadron approach, we can directly relate $\Pi_\sigma(\mathbf{p}', \mathbf{p}; \Gamma; \mu)$ to the Jones-Scadron form factors G_{M1} , G_{E2} and G_{C2} as follow:

$$\Pi_\sigma(\mathbf{0}, -\mathbf{q}; \Gamma_4; \mu) = iA \epsilon^{\sigma 4 \mu j} p^j G_{M1}(Q^2), \quad A = \sqrt{\frac{2}{3}} \frac{m_\Delta + m_N}{4m_N E_N} \sqrt{\frac{E_N}{E_N + m_N}} \quad (14)$$

$$\Pi_\sigma(\mathbf{0}, -\mathbf{q}; \Gamma_k; 4) = iB \left(\delta_{\sigma k} - \frac{3p_\sigma p_k}{\mathbf{p}^2} \right) \mathcal{G}_{C2}(Q^2), \quad B = \frac{\mathbf{p}^2}{2m_\Delta} A. \quad (15)$$

$$\begin{aligned} \Pi_\sigma(\mathbf{0}, -\mathbf{q}; \Gamma_k; j) = A \left\{ \frac{1}{2} (p_\sigma \delta_{kj} - p_k \delta_{\sigma j}) \mathcal{G}_{M1}(Q^2) \right. \\ \left. - \left[\frac{3}{2} (p_\sigma \delta_{kj} + p_k \delta_{\sigma j}) - \frac{3p_\sigma p_k p_j}{\mathbf{p}^2} \right] \mathcal{G}_{E2}(Q^2) \right. \\ \left. - \frac{(E_N - m_\Delta)}{2m_\Delta} p_j \left(\delta_{\sigma k} - \frac{3p_\sigma p_k}{\mathbf{p}^2} \right) \mathcal{G}_{C2}(Q^2) \right\}. \quad (16) \end{aligned}$$

where $\mathbf{q} = \mathbf{p} - \mathbf{p}'$ is the momentum transfer and $Q^2 = -q^2$. Following Ref [9] in order to extract the transition form factors, we construct linear combinations, $S_1(\mathbf{q}, \mu)$, $S_2(\mathbf{q}, \mu)$ and $S_3(\mathbf{q}, \mu)$ of the $\Pi_\sigma(\mathbf{p}', \mathbf{p}; \Gamma; \mu)$ for different choices of σ , Γ and μ to isolate the different form factors.

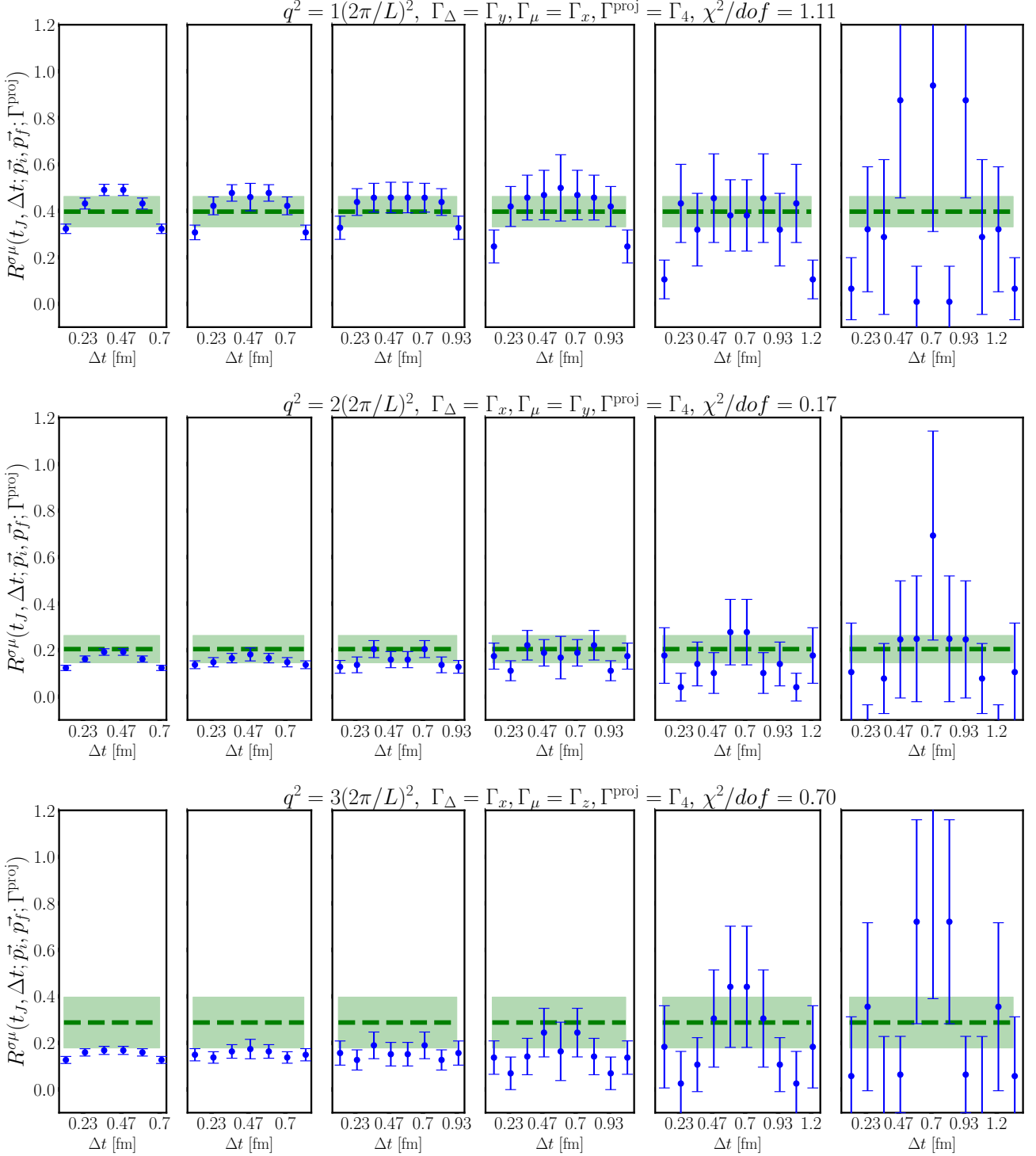


Figure 2: Preliminary fits for the ratio $R_{\sigma}^{\text{sym}}(t_2, t_1; \mathbf{p}', \mathbf{p}; \Gamma; \mu)$ as a function of the source-sink separation for nucleon momentum $\mathbf{p} = (0, 0, -1), (1, 0, -1), (1, 1, -1)$ and Δ momentum $\mathbf{p}' = (0, 0, 0)$. The current insertion is the time component of the vector current and the projection matrix is Γ_4 . The horizontal bands represent the results of the plateau fits to the central 3 time slices for 3 highest source-sink separations.

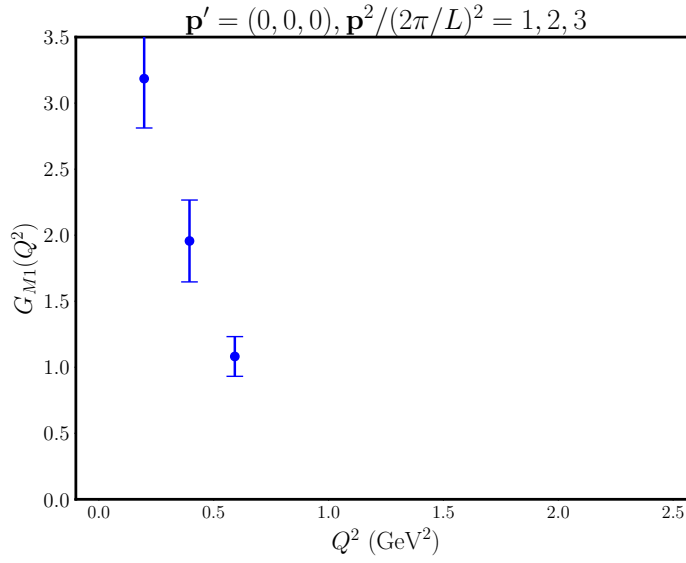


Figure 3: Preliminary results for the G_{M1} form factor as a function of Q^2 . The error bars represent the statistical uncertainties from the plateau fits.

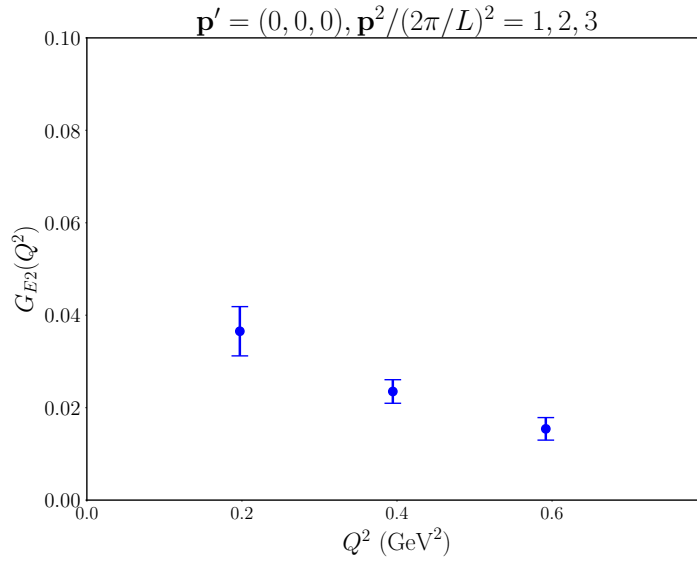


Figure 4: Preliminary results for the G_{E2} form factor as a function of Q^2 . The error bars represent the statistical uncertainties from the plateau fits.

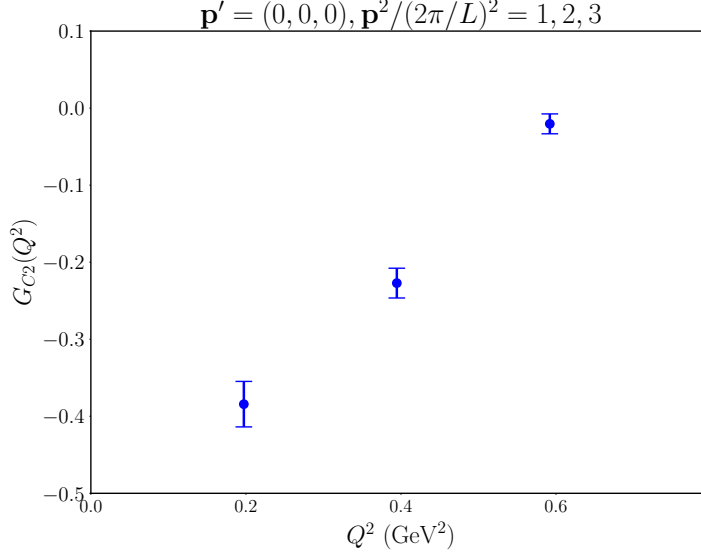


Figure 5: Preliminary results for the G_{C2} form factor as a function of Q^2 . The error bars represent the statistical uncertainties from the plateau fits.

3. Results

We extract the transition form factors for three different choices of the nucleon momentum $\mathbf{p} = (0, 0, -1)$, $(1, 0, -1)$, $(1, 1, -1)$ and Δ momentum $\mathbf{p}' = (0, 0, 0)$ to get three different values of Q^2 . The preliminary results for the G_{M1} , G_{E2} and G_{C2} form factors as a function of Q^2 are shown in Fig. 3, Fig. 4, and Fig. 5. The error bars represent the statistical uncertainties from the plateau fits. We observe that the signal quality for G_{M1} , G_{E2} and G_{C2} are good thus giving confidence for us to proceed with the multi-hadron analysis. There is reasonable agreement in the behavior of the form factors extracted here with Ref [10]. We also observe that the excited-state contamination is significant for the smaller source-sink separations, which highlights the importance of using multiple source-sink separations to control these systematics.

4. Outlook

In our future work, we will compute finite-volume matrix elements involving $N\pi$ interpolating operators at the source whose contraction topologies are shown in Fig. 6, and apply the BHWL formalism [15, 16] to extract the infinite-volume $N \rightarrow N\pi$ transition amplitudes.

Acknowledgments

This research used resources of the National Energy Research Scientific Computing Center (NERSC), a Department of Energy User Facility using NERSC award NP-ERCAP0035996. We thank Stefan Krieg and the BMW collaboration for providing the gauge configurations. S.P. was partially supported by DOE Grant KA2401045. L.L. acknowledges the project was financially supported by the Slovenian Research Agency through project N1-0360. S.M. is supported by the

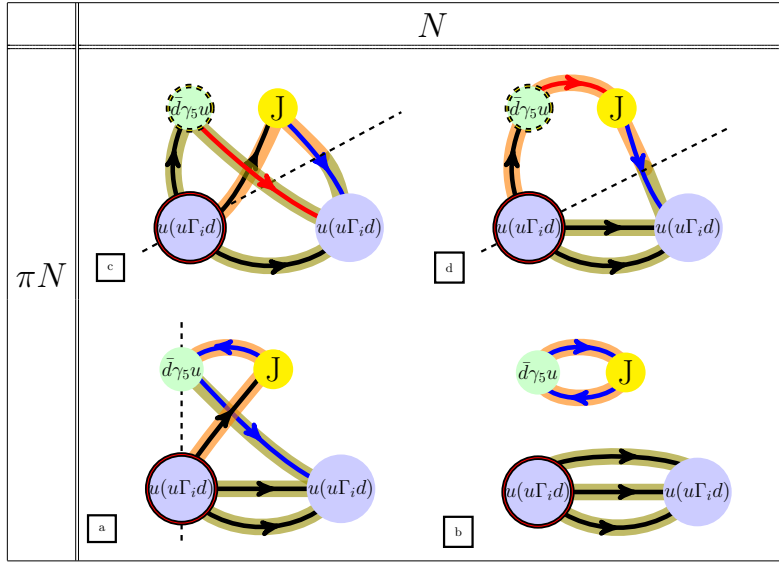


Figure 6: The three-point function topology for the multi-hadron approach. The point source is represented by the red bounded circle and the point-to-all propagator is represented by the blackline. The sequential source is the current insertion represented by the dashed green circle which represents the π at source and the sequential propagator is represented by the red line. The blue line represents the stochastic all-to-all propagator. The nucleon sink is represented by the blue circle. The dashed line represents the novel factorization strategy employed to reduce computational cost and reuse factors. The [b] topology employs one-end trick to compute the product of two stochastic all-to-all propagators.

U.S. Department of Energy, Office of Science, Office of High Energy Physics under Award Number DE-SC0009913. J.N. and A.P. acknowledge support by the U.S. Department of Energy, Office of Science, Office of Nuclear Physics under grants DESC-0011090 and DE-SC0018121 respectively. A.P. acknowledges support by the “Fundamental nuclear physics at the exascale and beyond” project under grant DESC0023116. The work of FP was supported by the projects PulseQCD, DeNuTra, MuonHVP(EXCELLENCE/0524/0269, EXCELLENCE/524/0455, EXCELLENCE/524/0017) co-financed by the European Regional Development Fund and the Republic of Cyprus through the Research and Innovation Foundation.

References

- [1] “V. Burkert at Nstar 2017.” <http://nstar2017.physics.sc.edu/talks/P11.pdf>.
- [2] “C. Roberts at Nstar 2017.” <http://nstar2017.physics.sc.edu/talks/P12.pdf>.
- [3] L. A. Ruso et al., *J. Phys. G* **52** (2025) 043001 [2203.09030].
- [4] CLAS collaboration, K. Joo et al., *Phys. Rev. Lett.* **88** (2002) 122001 [hep-ex/0110007].
- [5] A2 collaboration, W. J. Briscoe et al., *Phys. Rev. C* **100** (2019) 065205 [1908.02730].

- [6] C. Alexandrou, P. de Forcrand, H. Neff, J. W. Negele, W. Schroers and A. Tsapalis, *Phys. Rev. Lett.* **94** (2005) 021601 [[hep-lat/0409122](#)].
- [7] C. Alexandrou, G. Koutsou, J. W. Negele and A. Tsapalis, *Phys. Rev. D* **74** (2006) 034508 [[hep-lat/0605017](#)].
- [8] C. Alexandrou, T. Leontiou, J. W. Negele and A. Tsapalis, *Phys. Rev. Lett.* **98** (2007) 052003 [[hep-lat/0607030](#)].
- [9] C. Alexandrou, G. Koutsou, H. Neff, J. W. Negele, W. Schroers and A. Tsapalis, *Phys. Rev. D* **77** (2008) 085012 [[0710.4621](#)].
- [10] C. Alexandrou, G. Koutsou, J. W. Negele, Y. Proestos and A. Tsapalis, *Phys. Rev. D* **83** (2011) 014501 [[1011.3233](#)].
- [11] C. Chen, C. S. Fischer and C. D. Roberts, *Phys. Rev. Lett.* **133** (2024) 131901 [[2312.13724](#)].
- [12] G. Silvi et al., *Phys. Rev. D* **103** (2021) 094508 [[2101.00689](#)].
- [13] BMW collaboration, S. Durr, Z. Fodor, C. Hoelbling, S. D. Katz, S. Krieg, T. Kurth et al., , *JHEP* **08** (2011) 148 [[1011.2711](#)].
- [14] D. Drechsel and L. Tiator, *J. Phys. G* **18** (1992) 449.
- [15] R. A. Briceño, M. T. Hansen and A. Walker-Loud, *Phys. Rev. D* **91** (2015) 034501 [[1406.5965](#)].
- [16] R. A. Briceño and M. T. Hansen, *Phys. Rev. D* **94** (2016) 013008 [[1509.08507](#)].